Eur. Phys. J. A **3**, 129–132 (1998)

THE EUROPEAN PHYSICAL JOURNAL A

G–factor of the first 2^+ state in ^{180}Pt

F. Brandolini[1,a], N.H. Medina[1,2], A.E. Stuchbery[3], S.S. Anderssen[3], H.H. Bolotin[4], D. Bazzacco[1], D. De Acuña[5], M. De Poli[5], R. Menegazzo[1], P. Pavan[1], C. Rossi Alvarez[1], G. Vedovato[5]

[1] Dipartimento di Fisica dell' Universitá and INFN Sezione di Padova, Padova, Italy
[2] Instituto de Fisica, Universidade de São Paulo, São Paulo, Brazil
[3] Department of Nuclear Physics, Australian National University, Canberra, Australia
[4] School of Physics, University of Melbourne - Melbourne, Australia
[5] Laboratori Nazionali di Legnaro - INFN, Legnaro, Italy

Received: 14 May 1998 / Revised version: 7 July 1998
Communicated by C. Signorini

Abstract. The g–factor of the 2_1^+ state in ^{180}Pt has been measured by means of an implantation-decay technique in conjunction with the γ-ray detector array GASP, thereby extending the $g(2_1^+)$ systematics for Pt isotopes across the upper part of the valence neutron shell, beginning below mid-shell. Despite the variation in the number of valence neutron holes from 6 to 22, the g-factors remain nearly constant and near $0.7Z/A$.

PACS. 21.10.Ky Electromagnetic moments – 23.20.En Angular distribution and correlations measurements – 27.70.+q $150 \leq A \leq 189$

The low-excitation spectroscopy of the even platinum isotopes, ^{174}Pt through ^{198}Pt, provides one of the most studied, yet intriguing, cases of shape transition and shape coexistence phenomena [1] in atomic nuclei. While the stable isotopes ($A \geq 190$) are oblate [2,3], there is a transition to prolate shapes at about $N = 110$ (^{188}Pt). The nuclei $^{180-184}$Pt, near mid-shell ($N = 104$), have rotational-like ground-state bands associated with prolate deformation [3], while the lighter isotopes have irregular level sequences indicative of coexisting deformed and near spherical shapes (see [4,1] and references therein). Semi-empirical band-mixing calculations [4] reproduce the level structures and imply relatively large mixing between the strongly and weakly deformed states. Electric quadrupole transition rates in ^{184}Pt are consistent with this picture [5]. To understand shape mixing and the shape transition in the light transitional Pt isotopes at a more fundamental level, it is important to seek information concerning the underlying configurations of the coexisting structures. Measurements of g–factors may provide this information as the different shapes are believed to correspond to very different configurations [3].

The g–factors of the first 2^+ states in the even-even stable Pt isotopes have been accurately measured both at Australian National University (ANU) and at Legnaro National Laboratories (LNL) [6–8]. The values are quite constant as function of the number of neutrons, in contradistinction with Os stable isotopes, where a marked increase with the neutron number has been observed. Interacting boson model (IBM-2) calculations with a fixed number of bosons reproduce the systematics only for the Os isotopes [6], so that F–spin mixing has to be introduced [8,9] for the Pt isotopes. Pairing-plus-quadrupole model (PPQM) calculations predicted nearly constant g–factors for the stable isotopes of platinum and osmium, and decreasing g-factors for the neutron-deficient isotopes, in qualitative agreement with IBM-2 expectations [10].

A systematic study has been performed at the ANU, to extend the g–factor systematics to the unstable neutron-deficient Pt isotopes. Specifically, the g–factors of the 2^+ states in ^{184}Pt, ^{186}Pt and ^{188}Pt were measured relative to ^{192}Pt [11] and these were found to continue the near constant trend. The technique consisted in measuring the precession of γ-γ angular correlations for the cascades $0_2^+ \rightarrow 2_1^+ \rightarrow 0_1^+$, $3_1^+ \rightarrow 2_1^+ \rightarrow 0_1^+$, $4_1^+ \rightarrow 2_1^+ \rightarrow 0_1^+$ and $2_2^+ \rightarrow 2_1^+ \rightarrow 0_1^+$ in the nuclei of interest which were populated by β^+–decay of Au isotopes. The β^+-emitters were produced with a suitable heavy-ion fusion reactions using a chopped beam and the delayed γ–γ coincidences were observed in off-beam condition using a seven Ge detector array.

It is interesting to extend the measurements toward more neutron-deficient nuclei around $N = 100$ and to apply the technique with a larger multidetector array. In this work we report an investigation of the $N = 102$ nucleus ^{180}Pt. The measurement is more difficult than the previous ones owing to a lower fusion-reaction cross section

[a] *Mailing address:* Via F. Marzolo 8, I-35131 Padova, Italy, e-mail brandolini@pd.infn.it

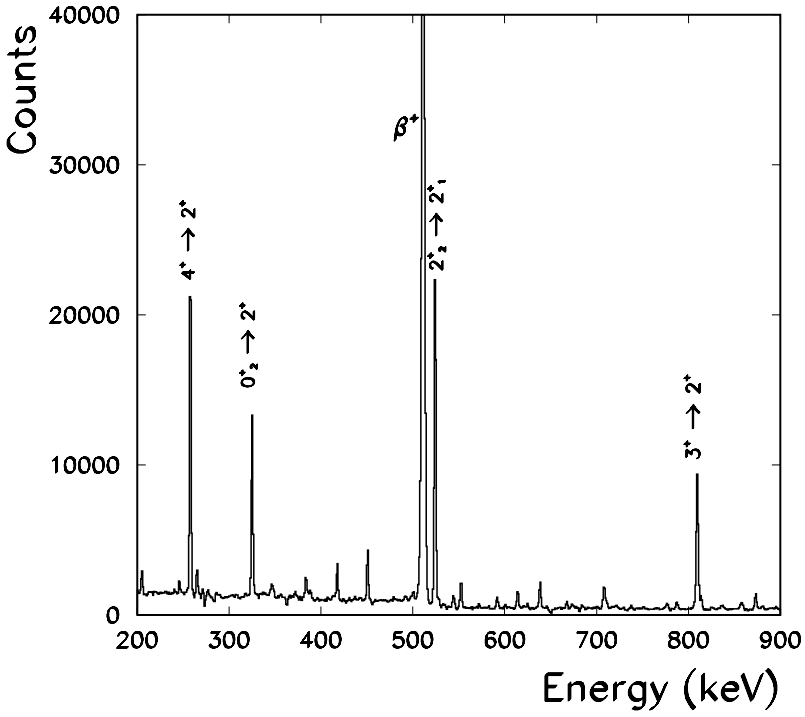

Fig. 1. Background subtracted coincidence γ–ray spectrum of ^{180}Pt gated on the $2^+ \rightarrow 0^+$ transition of 153 keV for all detector combinations for one field direction

and less favourable β-decay branching. Our study was undertaken at LNL with the GASP array composed of 40 Compton suppressed HPGe detectors of about 80% relative efficiency. The reaction ^{149}Sm(^{35}Cl,4n)^{180}Au was used at 168 MeV with an average beam current of 7 pnA and for about 2.5 days beam time. The target, kept at liquid nitrogen temperature, consisted of 1.2 mg/cm^2 of ^{149}Sm on a 4 mg/cm^2 Gd foil, and with a backing of 0.1 mm Au. To polarize the annealed Gd foil an external field of 0.045 T was produced by two NdFeB permanent magnets which were interchanged every 12 hours to reverse the field direction. The two magnets had a cylindrical shape and obscured two germanium detectors along a symmetry axis of the GASP array. Technical difficulties concerning the implementation of a rabbit system, as made in Ref. [11], in the GASP array for the short ^{180}Au lifetime (8.2 s) suggested the use of Gd as the ferromagnetic medium, which, in virtue of the higher Coulomb barrier, avoids the high γ-ray background that would come from fusion reactions on an iron layer.

A chopped beam with period T=52 μs and a duty cycle of about 75% was used. The γ–γ coincidences were accumulated only in off–beam conditions. The angular correlation was analysed in each of the 1406 useful detector combinations, by extracting the number of coincidences for gates on peak–peak, peak–background, background–peak and background–background, respectively. In this way 4 matrices (40×40) for the $0_2^+ \rightarrow 2_1^+ \rightarrow 0_1^+$ (324 keV $\rightarrow$ 153 keV) cascade were created from the list mode data, for each field direction. From these matrices the experimental angular correlation information has been condensed into a background subtracted peak–peak matrix, in the following referred as the angular correlation data, and one containing the propagated statistical error. The acquired background subtracted peak–peak coincidences in all detector combinations were about 1.2×10^4 for each field direction. As seen in Fig. 1, the cascades fed by the $3_1^+ \rightarrow 2_1^+$, $4_1^+ \rightarrow 2_1^+$, and $2_2^+ \rightarrow 2_1^+$ transitions do have a similar number of counts, but they were not useful for the present g–factor determination because the angular correlations have small slopes.

The hyperfine static field for Pt in Gd has been recently measured to be –38(5) T [12] from an integral IMPAC measurement following Coulomb excitation of ^{194,196,198}Pt. (Only a rather old determination of −78(12)T [13] was previously reported in a similar experiment; however the data for ^{196}Pt (and most likely ^{198}Pt) have since proved incorrect [12].) The hyperfine field for Pt in Gd is therefore considerably smaller than that for Pt in Fe, namely 113(9) T, obtained in the implantation-decay measurement on ^{192}Pt [15,11]. The smaller field for Gd hosts is not a real drawback since the long lifetime of the 2^+ state, τ= 540(50) ps [14], implies that the higher field value would give rise to a strong attenuation of the angular correlation. Of more concern is the fact that all of the implanted nuclei may not experience the same hyperfine field strength, as will be discussed later.

The unperturbed angular correlation observed for the $2_1^+ \rightarrow 0_1^+$ transition in the detector with index i in coincidence with the $0_2^+ \rightarrow 2_1^+$ transition observed in another detector with index j can be described as:

$$N_{ij} = A_0 + A_2 P_2(\theta_{ij}) + A_4 P_4(\theta_{ij}), \qquad (1)$$

where θ_{ij} is the angle between the detector directions.

Assuming that all implanted Pt nuclei experience the same static magnetic field B and referring the direction of the observed γ–rays to the direction of B, the P_l terms

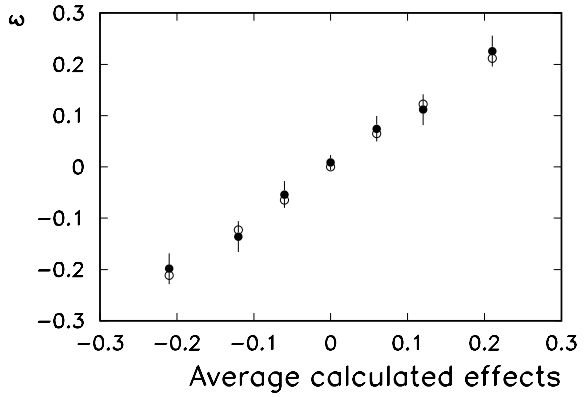

Fig. 2. Experimental effects ε (full circles) compared with calculated effects (open circles), after averaging in 7 groups of detector pair combinations, as explained in the text

for the perturbed angular correlation are given by:

$$P_l(\theta_{ij}) = P_l(\theta_i)P_l(\theta_j) + 2\sum_{m>0}\frac{(l-m)!}{(l+m)!}P_l^m(\theta_i)P_l^m(\theta_j) \times\frac{1}{\sqrt{1+(m\omega_L\tau)^2}}\cos m[(\varphi_i-\varphi_j)\pm\frac{\arctan(m\omega_L\tau)}{m}] \quad (2)$$

The Larmor frequency is defined as:

$$\omega_L\tau = -\frac{g\mu_N}{\hbar}B\tau$$

where the symbol $\pm$ refers to the alternate field directions 'up' ($\uparrow$) or 'down' ($\downarrow$). In the following, the effect ε_{ij} for each detector pair combination is defined from

$$\varepsilon_{ij} = \frac{N_{ij}^{\uparrow} - N_{ij}^{\downarrow}}{N_{ij}^{\uparrow} + N_{ij}^{\downarrow}}$$

where the coefficients N_{ij} are the angular correlation rates and indices i and j run from 1 to 40 with $i \neq j$ and excluding the indices of the two obscured detectors. It is stressed that the experimental effects do not depend on the γ–ray efficiency correction.

In order to obtain a good fit for all ε_{ij} effects simultaneously, it was found necessary to adopt a two-site model, as in [11], where a fraction of the implanted nuclei experience a low field (approximated as zero). In a first analysis the theoretical angular correlation coefficients, corrected for the attenuation caused by the finite solid angle of the γ–ray detectors, A_2/A_0=0.35 and A_4/A_0=1.06, were adopted. The best fit for the experimental data was obtained with $\omega_L\tau = 0.40(3)$ and a 0-field fraction of 30(5)% with a normalized χ^2 close to one. The good fit obtained points to the absence of systematic errors, as also illustrated in Fig. 2 where it is shown that experimental and the calculated effects agree very well. For a more convenient representation the 1406 experimental effects were plotted after averaging in 7 groups according to intervals of calculated effects: in fact, the calculated effects tend to cluster around 7 main average values due to the GASP geometry. One notes that the abscissa identifies the 7 groups of detector pairs according to these calculated average values, which also appear in the ordinate, so that they lie along a straight line.

The zero-field fraction is bigger than for Pt in Fe (about 10% [11]). One has to note that in the previous analysis the zero-field fraction strongly depends, as to some extent also the $\omega_L\tau$, on the assumption of unrelaxed angular coefficients, since the parameters are correlated in the analysis of effect data. In view of this and in order to get some more precise information about the zero-field fraction, it has been attempted to determine the experimental A_2 and A_4 coefficients directly from the angular correlation data N_{ij}, where much less parameter correlation is expected. However, in this case it proved difficult to obtain a sufficiently accurate efficiency correction and the normalized χ^2 was about three. A simultaneous fit of the effects and of the angular correlation for the 1406 detector combinations gives somewhat reduced coefficients, A_2/A_0=0.32(3) and A_4/A_0=0.80(9), which can be attributed to relaxation in the rather long lived state. With these fitted values of A_2 and A_4, $\omega_L\tau$ =0.38(3) and a 0-field fraction of 20(10)% were obtained. It may be noted that a higher 0-field component could be associated with a higher fraction of interstitial Pt nuclei due to the large atomic radius of Gd.

We have measured the precession $\omega_L\tau$ with a statistical precision of $\sim$ 8%, however the determination of the g factor from $\omega_L\tau$ requires further consideration. If one assumes that the average static field measured in [12] corresponds to a similar 0-field fraction of 20%, the static hyperfine field value to be considered when extracting the g–factor from $\omega_L\tau$ must also be increased appropriately. One should underline the need for caution, however, since in [12] the data were taken with the beam on, while in the present case they were delayed by several μs. On this longer time scale, some recovery of damage may occur, accompanied by a decrease in the 0-field fraction. Unfortunately, detailed information on this is not available for Pt in Gd. For Pt in Fe, the field observed in the implantation-decay measurement on ^{192}Pt is about 20% higher than that found for Pt in Fe from IMPAC measurements following Coulomb excitation [15,16]. To account for such effects qualitatively, the uncertainty in the adopted hyperfine field value was increased to 20%. In this way we obtain g = 0.32(6), the final uncertainty being dominated by the uncertainty in the absolute value of the hyperfine field.

As shown in Fig. 3, the g–factor is comparable with those found for ^{184,186,188}Pt [11]. We refer to [11] for detailed discussion of the g–factors in the neutron-deficient Pt isotopes, but briefly summarize the main points here. The IBM-2 prediction, with a fixed number of bosons, is shown in Fig. 3 as a point of reference. PPQM calculations [10] also predict similarly small g–factors near mid-shell that are not seen experimentally. Instead, the experimental results are close to $0.7Z/A$, as one would expect for prolate deformed nuclei in, for example, the Geometrical Collective Model [17].

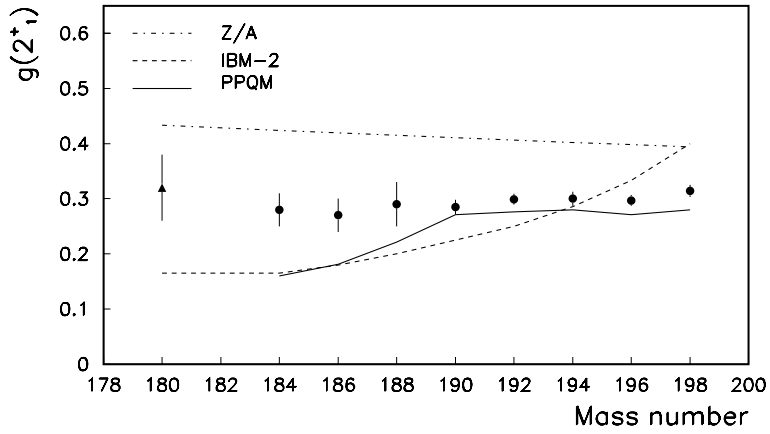

Fig. 3. Experimental g(2^+) in even Pt isotopes compared with theoretical predictions using the collective rotational value g_R=Z/A, the Interaction Boson Model (IBM–2) and the Pairing-Plus-Quadrupole Model (PPQM) [10]. The present experimental value is indicated as a full triangle

From a microscopic perspective, the deformed bands near mid-shell in the Pt isotopes are believed to be associated with an intruder (π $h_{9/2}$)^2 configuration, which drives the nucleus to a prolate shape and brings additional proton contributions to the g-factor. From this perspective, g–factor values in agreement with experimental results can obtained within a simple two-band mixing approach which estimates ≈70% dominance of the prolate configuration [11]. Essentially the same conclusions are reached whether the g–factors associated with the prolate and oblate shapes are taken from IBM–2 estimates, in which the deformed configuration has two extra proton bosons, or from Density-Dependent Hartree Fock calculations [18], in which the g-factors for weakly oblate shapes are small due to contributions from the $\nu i_{13/2}$ orbital.

In summary, we have measured the g–factor of the first excited state in ^{180}Pt by employing a novel implantation-decay technique in a large γ-ray detector array. The $g(2^+)$ values in the even Pt isotopes between ^{180}Pt and ^{198}Pt remain almost constant and near $0.7Z/A$. In view of changes in the structures of these nuclei and the contrasting behaviour of the g–factors in the neighbouring tungsten and osmium isotopes with similar neutron number, this is remarkable. We seem to have a deceptively simple outcome from subtle underlying microscopics that are still not fully understood.

We thank the staff of the LNL Tandem accelerator, and in particular dr. A. Facco, for providing a high quality pulsed beam. Mr. A. Buscemi is also acknowledged for the skilful technical assistance. This research was supported in part by the Australian Research Council. One of us (NHM) would like to acknowledge financial support from the brazilian agency CNPq (Conselho Nacional de Desenvolvimento Científico e Tecnológico).

References

1. J. L. Wood et al., Physics Reports 215 (1992) 101
2. G. J. Gyapong et al., Nucl. Phys. A 458 (1986) 165
3. R. Bengtsson et al., Phys. Lett. B 183 (1987) 1
4. G. D. Dracoulis et al., Phys. Rev. C 44 (1991) R1246
5. U. Garg et al., Phys. Lett. B 180 (1986) 319
6. A. E. Stuchbery, G. J. Lampard and H. H. Bolotin, Nucl. Phys. A 528 (1991) 447
7. F. Brandolini et al., Nucl. Phys. A 536 (1992) 366
8. S. S. Anderssen, A. E. Stuchbery, S. Kuyucak, Nucl. Phys. A 593 (1995) 212
9. S. Kuyucak and A.E. Stuchbery, Phys. Lett. B 348 (1995) 315
10. K. Kumar and M. Baranger, Nucl. Phys. A 110 (1968) 529
11. A. E. Stuchbery et al., Phys. Rev. Lett. 76 (1996) 2246
12. A. E. Stuchbery and S. Anderssen, Phys. Rev. C 51 (1995) 1017
13. G. M. Heestand et al., Phys. Rev. B 2 (1970) 3693
14. De Voigt et al., Nucl. Phys. A 507 (1990) 472
15. S. Anderssen and A. E. Stuchbery, Hyperfine Interact. 96 (1995) 1
16. A.E. Stuchbery, S.S. Anderssen and E. Bezakova, Hyperfine Interact. 97/98 (1996) 479
17. D. Troltenier, J. A. Maruhn, and W. Greiner, Z. Phys. A 338 (1994) 1
18. D. W. L. Sprung et al., Nucl. Phys. A 326 (1979) 37